

Photochemical Functionalization of Hydrogen-Terminated Diamond Surfaces: A Structural and Mechanistic Study

Beth M. Nichols,[†] James E. Butler,[‡] John N. Russell, Jr.,[‡] and Robert J. Hamers^{*,†}

Department of Chemistry, University of Wisconsin—Madison, 1101 University Avenue, Madison, Wisconsin 53706, and U.S. Naval Research Laboratory, 4555 Overlook Avenue, S.E., Washington, DC

Received: August 12, 2005; In Final Form: September 7, 2005

Hydrogen-terminated diamond surfaces can be covalently modified with molecules bearing a terminal vinyl (C=C) group via a photochemical process using sub-band-gap light at 254 nm. We have investigated the photochemical modification of hydrogen-terminated surfaces of nanocrystalline and single-crystal diamond (111) to help understand the structure of the films and the underlying mechanism of photochemical functionalization. A comparison of the rates of photochemical modification of single-crystal diamond and nanocrystalline diamond films shows no significant difference in reactivity, demonstrating that the modification process is not controlled by grain boundaries or other structures unique to polycrystalline films. We find that both single-crystal and polycrystalline hydrogen-terminated diamond samples exhibit negative electron affinity and are functionalized at comparable rates, while oxidized surfaces with positive electron affinity undergo no detectable reaction. Gas chromatography–mass spectrometry (GC-MS) analysis shows the formation of new chemical products in the liquid phase that are formed only when the alkenes are illuminated in direct contact with H-terminated diamond, while control experiments with other surfaces and in the dark show no reaction. Our results show that the functionalization is a surface-mediated photochemical reaction and suggest that modification is initiated by the photoejection of electrons from the diamond surfaces into the liquid phase.

Introduction

Diamond has many outstanding physical and chemical properties that make it a useful material in a wide range of applications.^{1,2} While the mechanical properties of diamond are well-known, many emerging applications are making use of the high chemical stability of diamond,³ which makes it an attractive material for applications that involve exposure to aqueous solutions, especially under physiological conditions.^{4,5} The chemical stability combined with semiconducting electrical properties makes diamond and diamond thin films attractive substrates in applications such as biological and chemical sensing.^{4,6,7} However, a thorough understanding of diamond surface chemistry has yet to be developed.⁸

By using reactions which are prevalent in synthetic organic chemistry as well as those used for modifying silicon surfaces, many different methods for diamond functionalization have been developed. These include reactions involving radical initiators such as organic peroxides,^{9,10} halogenation of diamond surfaces with subsequent organic functionalization,^{11–13} electrochemical reduction of diazonium salts,¹⁴ and photochemical terminations at varying energies (172 nm, 7.2 eV)¹⁵ (254 nm, 4.9 eV).^{16,17} By terminating the surface with molecules which have reactive groups at the exposed interface, further modifications such as DNA or protein attachment for use in sensing applications can be achieved.^{4,6,7,18,19}

Of particular interest is the photochemical reaction of diamond with alkenes under 254 nm light,^{4,16} as depicted in Figure 1. In this reaction, hydrogen-terminated nanocrystalline diamond films are covalently modified with molecules bearing a terminal vinyl

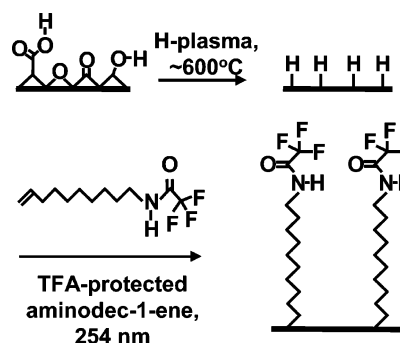


Figure 1. Reaction scheme for photochemical modification of diamond.

(C=C) group by way of a photochemical process.¹⁶ This reaction is intriguing because it uses 254 nm photons whose energy (4.9 eV) lies below the 5.5 eV bulk band gap of diamond; furthermore, several of the alkenes of interest are also nearly transparent at the 254 nm wavelength. While the photochemical modification of diamond has been shown to produce stable functional monolayers,^{4,5,19} many questions remain about how the reaction proceeds mechanistically and how the organic film is organized on the surface. Here, we report an investigation of the structure and mechanism of the photochemical modification of diamond with functionalized terminal alkenes.

Experimental Section

Sample Preparation. Nanocrystalline diamond thin films (p-type, B-doped, 0.49 μm thick) were grown on silicon (111) wafers at the Naval Research Laboratory with a boron concentration of $\sim 10^{18} \text{ cm}^{-3}$ following previously published procedures.²⁰ Natural single-crystal diamond (111) and (100), type IIb, were purchased from Harris International. All diamond

* Corresponding author. E-mail: rjhamers@wisc.edu.

[†] University of Wisconsin—Madison.

[‡] U.S. Naval Research Laboratory.

samples were cleaned in 3:1 HCl/HNO₃ (diluted 1:1 in H₂O) to remove contaminant metal species and 3:2 H₂SO₄/HNO₃ to remove graphitic and amorphous carbon prior to hydrogen termination. Samples were heated to ~600 °C in a 13.56 MHz inductively coupled hydrogen plasma (20 Torr H₂) for 5 min, cooled under plasma for 15 min, and brought back to room temperature under 5 Torr H₂ for 20–45 min. We note that cooling the sample with the plasma *on* is critical to achieving good hydrogen termination. Using X-ray photoelectron spectroscopy (XPS), the C(1s) and O(1s) core-level spectra were acquired; these show that the plasma treatment leaves a hydrogen-terminated surface with very little oxygen contamination.

The H-terminated samples were placed on quartz slides inside a Teflon reaction chamber. Small volumes (5–10 μL) of the liquid reactants were placed onto the diamond surface and covered with a second quartz slide, trapping a thin liquid film over the surface. The Teflon chamber was sealed with a quartz window, and the sample was illuminated with a low-pressure mercury lamp (254 nm, ~1 mW/cm²) under a flow of dry N₂. Reactions were allowed to proceed for varying times at room temperature. Most experiments reported here were performed using trifluoroacetamide-protected 10-aminodec-1-ene (TFAAD) that was synthesized and purified as previously described.²¹ Analysis of the starting material by gas chromatography–mass spectrometry (GC-MS) showed no detectable impurities. Some experiments were performed using perfluorodecene (3,3,4,4,5,5,6,6,7,7,8,8,9,9,10,10,10-heptadecafluoro-1-decene, Aldrich) and 1-dodecene (Aldrich). Analysis of these showed no significant impurities; they were used without further purification. After the photochemical reaction, diamond samples were sonicated in methanol (5 min) and chloroform (5 min) to remove any physisorbed reactants and dried with N₂ before analysis.

Characterization. The samples were characterized using XPS and ultraviolet photoelectron spectroscopy (UPS) in a single ultrahigh-vacuum system ($P < 5 \times 10^{-10}$ Torr) equipped with a load-lock for sample introduction, a monochromatized Al K α element (1486.6 eV) and He(I) emission lamp (21.2 eV) as excitation sources, and a hemispherical analyzer with a multi-channel detector. Analyzer resolutions of 0.05–0.1 eV and 0.1–0.2 eV were used for UPS and XPS measurements, respectively. Spectra were obtained immediately after each chemical processing step to avoid contamination. Unless otherwise noted, the measurement geometry involved collecting electrons ejected at 45° from the surface normal. Atomic area ratios for varying core-level spectra such as C(1s) and F(1s) will be denoted as $A_{F(1s)}/A_{C(1s)}$; these ratios were determined by fitting raw data to Voigt functions with a baseline correction and adjusting values for atomic sensitivity factors (C, 0.296; F, 1.00; N, 0.477; O, 0.711). In UPS measurements, samples were biased –1 to –2 V to ensure that the vacuum level of the sample was higher in energy than that of the analyzer; this is a requirement for obtaining accurate work function and electron affinity measurements.²² Spectra of tantalum clips in direct contact with the samples were obtained to determine the Fermi cutoff and adjust for differences in the sample and analyzer Fermi levels. UPS spectra presented here have been corrected for sample bias and the Fermi cutoff so that 0 eV corresponds to the Fermi energy, E_F .

Postreaction liquid-phase components were analyzed by GC-MS using an RTX-5 column. Samples were collected from the reaction cell using a methanol wash (~0.5 mL) of material from the diamond surface or quartz slide followed by dilution to constant volume in methanol. The methanol acts to provide a

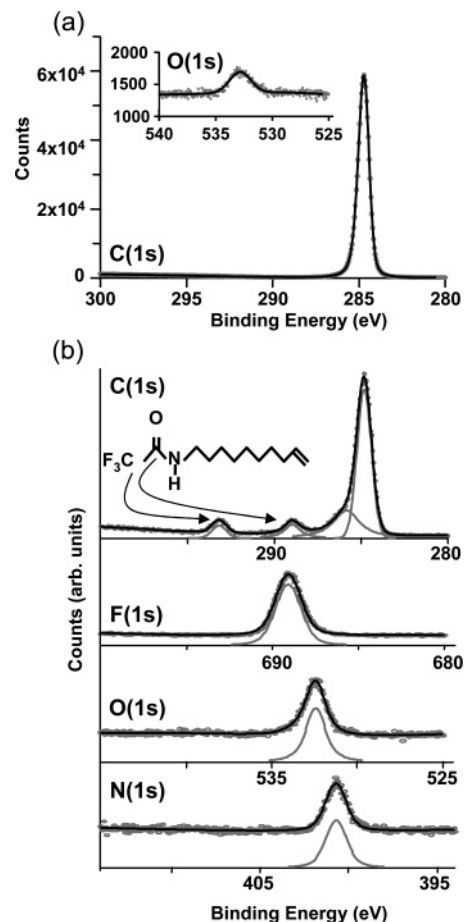


Figure 2. XPS spectra of (a) H-terminated NCD and (b) TFAAD terminated NCD. Individual spectra not to scale.

convenient marker peak in the GC spectra for normalization of the time axis.

Results

Quantitative Analysis of Surface Functionalization. Figure 2a shows a high-resolution XPS spectrum of the C(1s) and O(1s) regions of a hydrogen-terminated nanocrystalline diamond film (H–NCD). The spectrum shows a single, sharp peak at 284.5 eV with a full width at half-maximum (fwhm) of 0.9 eV, only slightly larger than the width of the monochromatized Al K α source. No features are evident at higher binding energies of ~286–290 eV, where oxidized carbon species would be observed. The sharp, symmetric shape of the peak indicates that the surface is free of non-diamond carbon impurities.²³ The inset shows the O(1s) region for the same surface, showing only very weak intensity. Measurement of the O(1s) and C(1s) peak areas leads to a ratio of areas, $A_{O(1s)}/A_{C(1s)}$, of 0.0059; after accounting for the C(1s) sampling depth as controlled by the inelastic mean free path, this corresponds to less than 0.1 monolayer (oxygen atoms per surface carbon atoms) for the H-terminated surface. XPS measurements on H-terminated single-crystal diamond (111) samples, H–(111) (natural IIB, cleaved face; not shown), are identical to those shown here, except for a slightly lower amount of oxygen on the diamond (111) samples. For both NCD and single-crystal diamond, we conclude that the H-termination procedure leaves a clean, hydrogen-terminated surface that is virtually free of oxidized sites or other contamination.

Figure 2b shows XPS spectra of the C(1s), F(1s), O(1s), and N(1s) regions of a nanocrystalline diamond surface after photochemical functionalization with TFAAD. The C(1s) peak

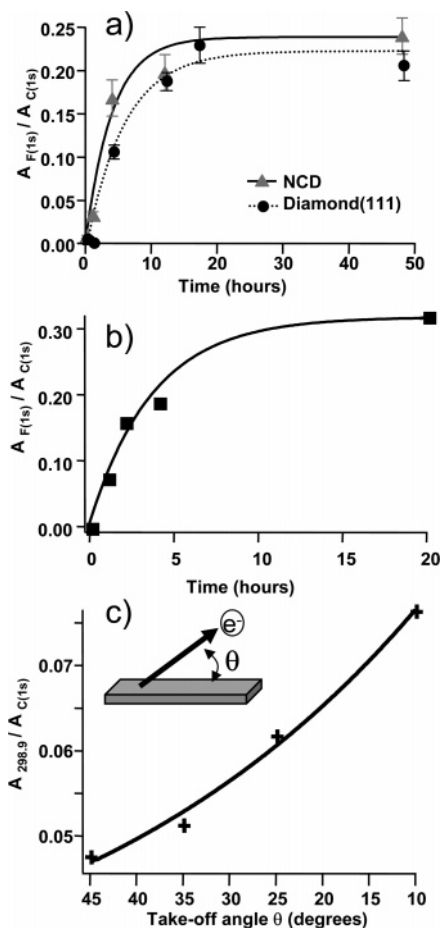


Figure 3. Functionalization of diamond surfaces with (a) TFAAD and (b) perfluorodecene (on NCD) as a function of illumination time. (c) Normalized intensity of the high binding energy C(1s) peak as a function of takeoff angle.

for the TFAAD-functionalized surface has a sharp peak at 284.5 eV, along with a significant shoulder at 286.1 eV and two satellite peaks at 288.7 and 292.9 eV. On the basis of electronegativity considerations, we attribute the peak at 292.9 eV to the C atom in the CF_3 group and the 286.1 eV peak to the carbonyl carbon.¹⁶ Quantitative measurements of the area of the F(1s), O(1s), and N(1s) peaks shown in Figure 2b yield area ratios of $A_{\text{F}(1s)}:A_{\text{O}(1s)}:A_{\text{N}(1s)} = 3.0:1.3:1.0$; these values correspond closely to the values of 3:1:1 expected from the molecular formula of TFAAD, $\text{C}_{12}\text{H}_{20}\text{F}_3\text{NO}$. The slightly higher amount of oxygen is likely due to the small amount of contaminant oxygen initially on the H-terminated sample. We thereby conclude that the attachment to the surface leaves the molecules intact and, in particular, does not lead to any detectable changes in the amine functionality or its protecting group.

To characterize the rate of functionalization, we monitored the reaction of TFAAD with H-NCD and H-(111) as a function of time, using the $A_{\text{F}(1s)}/A_{\text{C}(1s)}$ ratio as a measure of the extent of surface termination. For the NCD sample, the $A_{\text{F}(1s)}/A_{\text{C}(1s)}$ ratio, shown in Figure 3a, increases linearly at first and then reaches a limiting value of 0.24 after ~ 15 h. To identify whether grain boundaries of the polycrystalline film significantly influence the surface reactivity, we conducted similar experiments using single-crystal samples (p-type, boron-doped, type IIB) that were H-terminated and then modified using the same procedures. Figure 3a shows that on the diamond (111) surface the $A_{\text{F}(1s)}/A_{\text{C}(1s)}$ ratio has a time dependence nearly identical to that observed on the polycrystalline sample, with the $A_{\text{F}(1s)}/A_{\text{C}(1s)}$

ratio reaching a limiting value of 0.22. Identical measurements on a diamond (100) sample (not shown) yield a limiting $A_{\text{F}(1s)}/A_{\text{C}(1s)}$ ratio of 0.24 (reaction time = 22 h). The limiting $A_{\text{F}(1s)}/A_{\text{C}(1s)}$ ratios on the single-crystal diamond (111) and (100) samples and on the NCD sample are identical within experimental error. This similarity as well as the similarity in rate of functionalization between single-crystal and NCD samples shows that grain boundaries of the NCD sample do not control its reactivity.

While H-terminated samples can be easily functionalized, oxidized samples show little or no reactivity toward alkenes. The Supporting Information includes XPS data of an oxidized diamond sample that was exposed to TFAAD and illuminated at 254 nm. Even after extended periods of time, no reaction is observed with oxidized diamond surfaces.

Most experiments reported here were performed using TFAAD, which exhibits some absorption at 254 nm due to the TFA protecting group. To verify that photochemical functionalization does not involve direct excitation of the $\text{C}=\text{C}$ functionality, we obtained XPS data for the photochemical reaction of $\text{H}_2\text{C}=\text{CH}-\text{C}_8\text{F}_{17}$ (perfluorodecene), which has virtually no absorption at 254 nm, with H-NCD. Figure 3b shows that the resulting time dependence is nearly identical to that of the TFAAD. Other studies have demonstrated functionalization with several different terminal alkenes, including 1-dodecene ($\text{HC}=\text{CH}-\text{C}_{10}\text{H}_{21}$), that are transparent at 254 nm, while saturated alkanes show little or no detectable reactivity.^{16,23} The present and previous data demonstrate that the photochemical functionalization is a general reaction that works for a wide variety of molecules having an alkene functionality but does not depend on the molecule of interest having a strong absorption at the wavelength of excitation.

Structure of Monolayer Films. The covalently bound TFAAD on the single-crystal (111) surface was analyzed using angle-resolved XPS (AR-XPS). Extracting quantitative information on diamond is difficult because the C(1s) signal intensity arises from both the diamond bulk and the TFAAD layer. The area of the high binding energy C(1s) peak at 292.2 eV (from the CF_3 group) relative to the total C(1s) area can be used as a measure of the molecular density. Figure 3c shows the $A_{292.2}/A_{\text{C}(1s)}$ ratio as a function of photoelectron takeoff angle for a TFAAD-terminated diamond (111) surface. The $A_{292.2}/A_{\text{C}(1s)}$ ratio is approximately 0.047 at an angle of 45° , increasing to approximately 0.075 at an angle of 80° from the normal (10° from the sample plane). Because of the inability to distinguish the underlying diamond bulk from the alkyl chain, it is not possible to accurately determine the molecular density directly from these data. However, a *minimum* can be set if it is assumed that all C(1s) intensity at lower binding energies arises from the diamond and not from the organic layer. In this case, the number of carbon atoms that are detected can be determined separately from the known electron attenuation length (1.18 nm)^{24,25} and using the density of diamond (3.51 g/cm³) and the 45° geometric angle, yielding 4.2×10^{15} atoms/cm². The ratio $A_{292.2}/A_{\text{C}(1s)} = 0.047$ then yields $\sim 1.9 \times 10^{14}$ TFAAD molecules/cm². This number is a lower limit because in reality the C(1s) signal includes contributions from both the molecular layer and the underlying diamond substrate.

The angular dependence shows that the relative contribution from the CF_3 groups increases at takeoff angles close to the sample plane. This is consistent with the CF_3 groups being at the exposed interface. We further note that previous studies using this same molecule^{4,19} have shown that after photochemically linking to the diamond surface, subsequent chemical

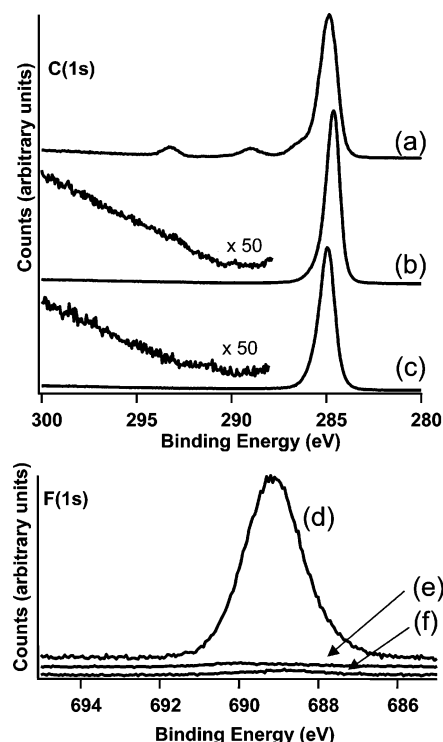


Figure 4. Functionalization of the H–NCD surface with TFAAD using various illumination sources: (a, d) 4 h, 254 nm (4.9 eV), ~ 1 mW/cm²; (b, e) 4 h, 325 nm (3.8 eV), 15 mW/cm²; (c, f) 22.5 h, dark.

processing steps to remove the trifluoroacetic acid protecting group proceed with high efficiency and minimal change in the N(1s) signal from the amine; these results demonstrate that the CF₃ groups are chemically accessible and therefore are almost certainly exposed at the outermost part of the molecular layer. On the basis of the comparison of our data to these results, we conclude that the photochemical functionalization leads to a self-terminating monolayer bonded to the diamond surface via the vinyl (C=C) group.

Mechanism. One surprising aspect of the photochemical modification is that it is initiated by light having a wavelength of 254 nm. Since the 4.9 eV energy of these photons is less than the 5.5 eV bulk band gap of diamond²⁶ and is also below the onset of absorption in most molecules containing only one C=C functionality, the mechanism of the photochemical modification has remained unclear. To help determine the mechanism of reaction, we have performed a variety of experiments to help identify the roles of the surface and of the liquid-phase reactants in controlling the functionalization.

Photon Energy Dependence. To help establish the factors affecting the functionalization, we characterized surfaces that were only *partially* functionalized with TFAAD and compared these with several other samples. We first prepared an H–NCD sample and partially functionalized it with TFAAD by illuminating it with 254 nm (~ 1 mW/cm²) for 4 h. XPS of this partially terminated sample yielded an area ratio $A_{F(1s)}/A_{C(1s)} = 0.17$, below that of the fully functionalized surface. The C(1s) spectrum, shown in Figure 4a, has the usual sharp peak at 284.5 eV associated with the bulk diamond and the alkyl chain, along with the additional peaks at 288.7 and 292.9 eV from the carbonyl and CF₃ groups of the TFA protecting group. The F(1s) spectrum is shown in Figure 4d. The C(1s) and F(1s) spectra are consistent with a diamond sample partially modified with the TFAAD molecule.

A second, identical H–NCD sample was exposed to TFAAD for 22.5 h in total darkness and then cleaned using procedures

identical to those used with the photochemically treated samples. The C(1s) spectrum (Figure 4b) has a single, sharp peak at 285 eV, with no evidence for peaks near 289 or 293 eV that would be characteristic of covalently linked TFAAD. The F(1s) signal (Figure 4e) is extremely weak, giving a $A_{F(1s)}/A_{C(1s)}$ of only 0.0081; this value is less than 5% of the value of 0.17 that was observed on the sample partially terminated under 254 nm light. The absence of high-energy C(1s) peaks and the low $A_{F(1s)}/A_{C(1s)}$ indicate that H–NCD does not react with TFAAD in the dark.

In addition to emission at 254 nm, low-pressure Hg lamps produce a small amount of emission at 185 nm (6.0 eV). To identify whether these short-wavelength photons are responsible for the photochemical modification, we conducted experiments in which samples were illuminated through a filter that absorbs all light below 220 nm. This filter had no significant effect on the rate of photochemical modification, leading us to conclude that the functionalization is induced by the 254 nm photons.

We also investigated whether lower energy photons could induce the photochemical reaction. Because there are few tunable sources of excitation with sufficient intensity at short wavelengths, we used a line source at 325 nm (3.8 eV, ~ 10 mW/cm²) produced by a HeCd laser (Omnichrome 2056-8/25M). Figure 4c shows the C(1s) spectrum of a sample that was covered with TFAAD and then illuminated for 4 h with this source. It shows only a single peak at 285 eV, with no evidence for significant reaction with the surface. Measurement of the F(1s) intensity, shown in Figure 4f, yields an $A_{F(1s)}/A_{C(1s)}$ ratio of 0.0076. This value is less than 5% of that observed on the surface illuminated with 254 nm light for 4 h and similar to the value observed for the “dark” control. The C(1s) and F(1s) data both show that even though the 325 nm source has an intensity (10 mW/cm²) ~ 10 times that of the 254 nm source (1 mW/cm²), the longer wavelength does not induce any significant reaction. Accordingly, we conclude that 3.8 eV photons are not sufficiently energetic to allow the reaction to progress.

Valence-Band Structure of Diamond Samples. One very interesting property of diamond is that many studies have reported that H-terminated surfaces of diamond (111) and diamond (100) exhibit negative electron affinity (NEA), while “clean” (vacuum-annealed) and oxidized surfaces have positive electron affinities.^{27–31} NEA refers to the situation in which the vacuum level is lower in energy than the conduction band minimum. The existence of NEA in a vacuum has implications for the mechanism of reaction, as previous studies have demonstrated that NEA diamond surfaces can emit electrons when illuminated, even using sub-band-gap light.^{32–35} Because the possible existence of NEA on *nanocrystalline* diamond has not been established previously, we investigated the valence band electronic structure of diamond samples.

Parts a–c of Figure 5 show UPS spectra for H–NCD and H–NCD samples that were partially ($A_{F(1s)}/A_{C(1s)} = 0.04$) and fully photochemically terminated ($A_{F(1s)}/A_{C(1s)} = 0.26$) with TFAAD. Parts d–f of Figure 5 show these same spectra enlarged in the region near the Fermi energy. The H-terminated sample (Figure 5a) shows a broad band of states between 5 and 12 eV with a shoulder near 10 eV and a pronounced peak at 8.4 eV below the Fermi energy that is characteristic of the p-states of diamond.³⁶ The samples that were partially and completely modified with TFAAD (Figure 5b,c) show similar features overall. However, these surfaces differ significantly at energies near E_F . In particular, H–NCD and the surface partially modified with TFAAD both show an observable tail in the photoelectron spectrum up to the Fermi energy, while the surface

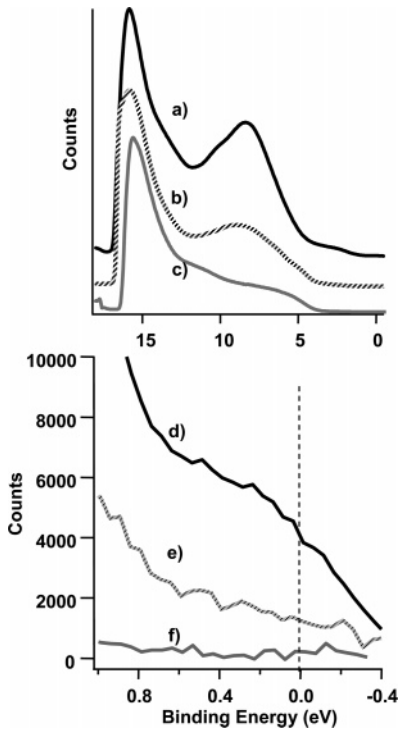


Figure 5. UPS of (a, d) H-terminated NCD, (b, e) an H-terminated NCD sample after partial modification with TFAAD, and (c, f) a H-terminated NCD sample after complete functionalization with TFAAD.

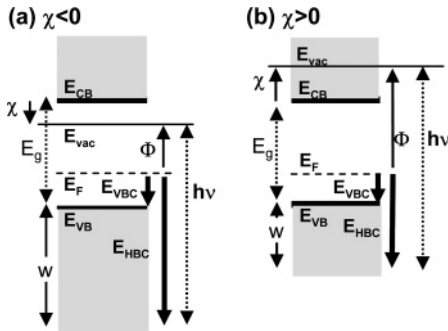


Figure 6. Energy band level diagrams for (a) a negative electron affinity surface and (b) a positive electron affinity surface.

that has been completely functionalized with TFAAD shows a very low photoelectron intensity near E_F (Figure 5d–f). These results show that the H-terminated surfaces have a significant density of electronic states within the bulk band gap slightly below E_F .

Figure 6 depicts the various energy levels involved in calculating the work function and electron affinity of these surfaces. It is necessary to determine the energy of the cutoff in electron yield at high binding energies, referred to as the high binding-energy cutoff (E_{HBC}), and the energy of the valence band edge, referred to as the valence-band cutoff (E_{VBC}). These energies were determined by fitting the data near 16–17 eV (E_{HBC}) and 1–2 eV (E_{VBC}) to a line and extrapolating to zero intensity. Because mid-gap surface states can obscure the valence band edge, we also separately measured the valence-band cutoff by measuring the position of the p-band and using a fixed 7.8 V offset between this peak and the valence-band cutoff.³⁷ Both methods yield nearly identical values. The work function, defined as the energy from E_F to the vacuum level, is $\Phi = h\nu - E_{HBC}$. The electron affinity is then $\chi = (h\nu - E_g) - (E_{HBC} - E_{VBC}) = (h\nu - E_g) - w$, where w , the emission width,

TABLE 1: Valence Band Cutoff Energy, Work Function, and Electron Affinity of Selected Surfaces

surface	E_{VBC} (eV)	ϕ (eV)	χ (eV)
H-terminated NCD	0.74	4.3	-0.5
H-terminated (111)	1.2	4.0	-0.3
partially TFAAD-modified NCD	0.86	4.4	-0.2
completely TFAAD-modified NCD	0.97	4.7	+0.2
H-NCD illuminated at 254 nm in ultrahigh vacuum	0.67	4.4	-0.4
annealed NCD (~1100 °C)	0.95	4.7	+0.2
annealed (111) (~1030 °C)	0.88	4.9	+0.3
oxidized (111)	0.96	4.8	+0.3

is defined as the range of energies over which significant electron emission is observed: $w = E_{HBC} - E_{VBC}$.

Analysis of the data in Figure 5 shows that the H–NCD has a valence band maximum at 0.74 eV below E_F and an E_{HBC} of 17.0 eV; these values yield $\Phi = 4.3$ eV and $\chi = -0.5 \pm 0.1$ eV. Similar measurements of H–(111) give an electron affinity of -0.3 eV, consistent with previous studies on single-crystal (111) and (100) surfaces.^{38,39} Perhaps more importantly, our data show that H–NCD also exhibits NEA. The value of $\chi = -0.5 \pm 0.1$ eV suggests that it should be possible to eject electrons from the valence band into vacuum using sub-band-gap photons of approximately $E_g - \chi \sim 5.0 \pm 0.1$ V. Moreover, since our valence band photoemission measurements show a significant density of occupied states between E_F and the valence band on H–NCD, it is clear that 254 nm photons (4.9 eV) have sufficient energy to excite electrons from these states to the conduction band, from which they can then be ejected into vacuum.

To determine how the electron affinity changes as the H-terminated surface was progressively functionalized with TFAAD, we performed similar measurements on the samples that were only *partially* terminated ($A_{F(1s)}/A_{C(1s)} = 0.04$, 2 h illumination) and fully terminated ($A_{F(1s)}/A_{C(1s)} = 0.26$) with TFAAD, described above and shown in Figure 5b,c. The electron affinity of the partially TFA-modified sample is still negative, -0.2 ± 0.1 eV, as shown in Table 1. After complete functionalization with TFAAD, the electron affinity of diamond becomes slightly positive, $+0.2 \pm 0.1$ eV.

While H-terminated samples can be easily functionalized photochemically, XPS measurements (data presented in Supporting Information) show that oxidized samples exhibit little or no photochemical reactivity; UPS measurements on these samples show a positive electron affinity, $\chi = 0.3 \pm 0.1$ eV.

To investigate whether 254 nm photons induce cleavage of C–H bonds at the surface of H-terminated diamond, we used UPS to look for the presence of carbon “dangling bonds”. Previous studies have shown that heating H-diamond above 900 °C removes hydrogen,⁴⁰ leading to a pronounced increase in the density of mid-gap states detected with UPS and an increase in the electron affinity.⁴¹ We conducted similar experiments on NCD and diamond (111) samples and, after ultrahigh-vacuum annealing, observed a pronounced increase in the density of states and an increase in the electron affinity to $\chi = 0.2 \pm 0.1$ eV (NCD) and $\chi = 0.3 \pm 0.1$ eV (diamond (111)), as shown in Table 1. These values are similar to values of $\chi \approx 0.4 - 0.5$ eV measured previously on diamond (111) samples after annealing in ultrahigh vacuum to desorb surface hydrogen.^{30,42} Thus, removal of hydrogen by heating leads to clearly identifiable changes in the valence band structure. To identify whether 254 nm light removes surface hydrogen directly, we illuminated H–NCD in the ultrahigh-vacuum XPS/UPS system through a quartz window for 15 h using the same lamp and lamp–sample distance as in other experiments. The resulting spectra showed

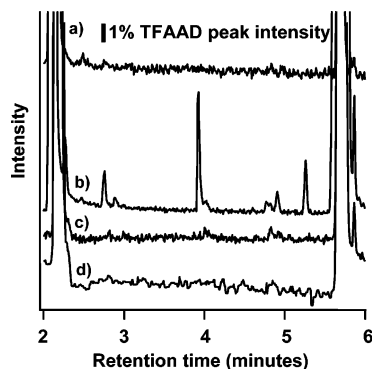


Figure 7. Gas chromatograms of TFAAD after various treatments: (a) neat TFAAD; (b) after 4 h exposure to UV on H–NCD; (c) after 4 h exposure to UV on quartz; (d) after 24 h dark exposure on H–NCD. All intensities were normalized to that of the main TFAAD peak at 5.8 min.

no detectable change before and after illumination. This is in quite striking contrast to the behavior observed when a sample is annealed. At a binding energy of 0.3 eV below E_F , which is within the bulk band gap on all samples, annealing H–NCD to remove the hydrogen increases the emission intensity by a factor of 2.5; however, when H–NCD was illuminated for 15 h the emission at this energy changed by less than 15%, which we estimate to be the noise level of the measurement. Similarly, quantitative measurement of the electron affinity and work function showed no change upon illumination in ultrahigh vacuum, as shown in Table 1. These data suggest that the 254 nm light does not result in significant loss of hydrogen from the surface via direct C–H bond cleavage.

Analysis of Solution-Phase Reaction Products. Previous studies have demonstrated that NEA surfaces of H-terminated diamond will eject electrons into vacuum when illuminated, even using sub-band-gap photons in the range of energies used in our experiments.^{32–35} Thus, our observation of NEA on H-terminated NCD and single-crystal diamond surfaces raises the possibility that electron ejection may have a role in controlling the surface reaction process. Moreover, because the solvation of an electron in a dielectric (i.e., polarizable) medium always lowers its energy, it should take less energy to eject an electron from diamond into a liquid (such as TFAAD) than it does to emit an electron into vacuum; this emission of electrons from a substrate into an overlayer is sometimes referred to as “internal photoemission” and has been shown previously to initiate electron-induced chemical reactions of molecules on metals⁴³ and on semiconductors.^{44,45}

To investigate whether electron emission creates new reaction products in the liquid phase, we used GC-MS to analyze the composition of the fluid medium before and after the photochemical modification. Data were first obtained for the TFAAD and the high-purity methanol that was used for rinsing. The chromatogram of methanol shows a single peak at \sim 2.2 min retention time. The chromatogram for the unreacted TFAAD (never illuminated or exposed to diamond) that was diluted in methanol is shown in Figure 7a. Two peaks, one at 2.2 min due to the methanol and a second at 5.8 min due to the TFAAD, are observed (shown off-scale to facilitate comparison of spectra). In the gas chromatogram of the TFAAD in methanol (Figure 7a), no impurity or byproduct peaks are observed that rise above \sim 1% of the height of the parent TFAAD peak.

Figure 7b shows the chromatogram of the TFAAD after photochemical reaction with the H–NCD sample. The liquid TFAAD was dripped onto the H–NCD, covered with a diamond-coated quartz window to form a thin liquid layer, and

illuminated with 254 nm light for 4 h under dry N_2 . The liquid that remained after the photochemical reaction was collected by rinsing the diamond surfaces with a small volume (\sim 50 μ L) of methanol and diluting to \sim 0.5 mL; Figure 7b shows the resulting gas chromatogram. In addition to the two large peaks with retention times of 2.2 and 5.8 min, the chromatogram shows new peaks at retention times of 2.4, 2.8, 4.0, 4.8, and 5.4 min. The mass spectrometric fragmentation patterns for these new product peaks (not shown) are too complex for detailed analysis. However, the relatively short retention times indicate that these products have molecular weights lower than the parent TFAAD molecule; we see no evidence for polymers, which would be expected to have longer retention times. Similar experiments on H-terminated diamond powders and H-terminated diamond (111) generated byproducts with identical retention times and similar product peak height ratios to those shown for the H–NCD. These experiments clearly demonstrate that new chemical species are present in the liquid phase after the photochemical reaction with diamond.

Two additional control experiments were performed. In the first, a small quantity of TFAAD was placed between two disks of polished quartz and illuminated for 4 h. A second, “dark” control was also prepared in which TFAAD was dripped onto H–NCD and kept under dry N_2 for $>$ 24 h in the dark. Chromatographic analyses of the collected liquid from these samples (Figure 7c,d) show only the two peaks at 2.2 and 5.8 min that arise from the methanol and TFAAD reactant, with no evidence for other products; the TFAAD does not undergo any chemical changes upon exposure to only 254 nm light or only H-diamond. As an additional point of reference GC-MS data were obtained of the liquid collected after oxidized diamond was exposed to TFAAD under 254 nm illumination. The resulting data (see Supporting Information) show no detectable changes in the fluid composition. These experiments establish that new chemical products are produced in the liquid phase upon illumination of hydrogen-terminated diamond samples with 254 nm light. Consequently, these products can only be formed via a photochemical reaction that directly involves the diamond.

While reported here for TFAAD, similar experiments performed using 1-dodecene as a reactant also show that photochemical illumination produces reaction products in solution (not shown). A previous study has shown that H-terminated diamond can be functionalized with dodecene, and that the functionalization can be detected via subtle changes in the shape of the C(1s) spectrum.²³ The observation of photochemical products in dodecene is significant because dodecene has a simpler molecular structure and has almost no absorbance at 254 nm, thereby eliminating any possibility of chemical changes in the liquid phase under 254 nm light. Thus, we conclude that the formation of new reaction products in the liquid phase is not unique to TFAAD but is a more general phenomenon associated with the photochemical functionalization.

Additional experiments were performed to identify whether the photochemical reaction rate could be altered by addition of a stronger electron acceptor, nitrobenzene, to terminal alkenes in solution, under the hypothesis that the added molecule would scavenge electrons ejected from the surface away from the alkene. These experiments, described in Supporting Information, showed no significant difference in the initial reaction rate between pure perfluorododecene and 95% perfluorododecene + 5% nitrobenzene, but were complicated by reaction of the nitrobenzene with the diamond surfaces.

Discussion

Physical Structure of Monolayer Films. Our XPS data show that functionalization of nanocrystalline diamond and single-crystal diamond with TFAAD occur at the same rate and that the reaction on both samples eventually self-terminates, yielding nearly identical $A_{F(1s)}/A_{C(1s)}$ area ratios of 0.24 and 0.22. This demonstrates that properties unique to polycrystalline films, such as grain boundaries, do not control the overall surface reactivity. A previous study showed that functionalization occurs with a variety of molecules bearing an alkene (C=C) functionality, but not with the saturated molecular analogues¹⁶ indicating that the C=C group greatly facilitates the functionalization reaction.

For bifunctional molecules it is possible that other functional groups, in addition to the C=C group, might affect the reactivity. This is particularly true for TFAAD, as this molecule has some absorption at 254 nm from the protecting group. However, three pieces of evidence indicate that the TFAAD protecting group does *not* directly participate in the reaction with the diamond surface. First, Figure 3 shows that the time dependence of the functionalization using TFAAD is quite similar to that using perfluorodecene, and these are also similar to that observed in our previous study using an alkene bearing the trifluoroethyl ester of a carboxylic acid.¹⁶ Thus, we conclude that, at least for these simple molecules, the photochemical functionalization is not strongly dependent on the details of molecular structure provided the alkene functionality is present. Second, the angular dependence of the $A_{292.2}/A_{C(1s)}$ data from TFAAD indicates that the fluorine groups are at the topmost (exposed) surface, thereby implying that the reaction occurs almost exclusively through the terminal C=C group. Finally, previous experiments from our laboratory⁴ and by others¹⁹ have demonstrated that the TFA protecting group can be removed to expose primary amine groups which can be used in subsequent reactions that are highly specific for primary amines. These data all strongly indicate that the functional groups associated with the TFA are spectators during the photochemical reaction.

From the XPS data, we find that the TFAAD binds such that there are at least 2×10^{14} molecules/cm². Since this analysis assumed that the main C(1s) peak at ~ 284.5 eV arises only from the diamond substrate and neglects the contribution from the alkyl chains, the true molecule density must be higher than this minimum value. This molecular density is somewhat smaller than the number of carbon atoms exposed on the diamond (111) and (100) surfaces, 7.8×10^{14} and 6.8×10^{14} atoms/cm², respectively. However, measurements of functionalized silicon surfaces have yielded molecular densities of $\sim 3.4 \times 10^{14}$ molecules/cm²,⁴⁶ and self-assembled monolayers on gold yielded $\sim 4.4 \times 10^{14}$ molecules/cm²,⁴⁷ for adsorbates with similar numbers of carbon atoms. The similarity between these values and our data suggests that the overall density is controlled by the packing and not by the availability of surface sites or changes in surface electronic properties (such as electron affinity) during functionalization.

Mechanism of Initiation. An intriguing aspect of the photochemical modification of diamond is the use of sub-band-gap illumination to initiate the reaction. New products are formed in the liquid phase after H-terminated diamond surfaces are illuminated in direct contact with the reactive alkenes (TFAAD and dodecene). In contrast, no products are observed when the liquid is illuminated in contact with quartz or oxidized diamond, nor on samples left in contact with diamond in the dark. These observations lead us to conclude that the surface functionalization must involve a photochemical reaction that is mediated by the H-terminated diamond, leading to functional-

ization of the surface and detectable chemical changes in the liquid phase.

Since surface “dangling bonds” on other semiconductors such as silicon are known to be reactive toward alkenes, we consider first the possibility that UV illumination cleaves C–H bonds at the diamond surface, creating surface radicals (“dangling bonds”), which could initiate reactions with molecules in the liquid phase. When we illuminated the H-terminated surface in our ultrahigh-vacuum system for as long as 15 h, the UPS spectrum did not show any detectable change. Since the removal of surface hydrogen by thermal annealing creates a very significant change in the UPS spectrum, this suggests that the extent of any UV-induced C–H bond cleavage is insignificant. This is consistent with the fact that while hydrocarbons have homolytic C–H bond cleavage energies of 4.1–4.3 eV,⁴⁸ photochemical C–H bond cleavage requires much higher energies (e.g., 7.2 eV for *n*-butane).

The liquid-phase analyses also help to distinguish between C–H cleavage and electron-induced processes. Using a rough analysis of the amount of material detected in our GC-MS studies, we estimate that the amount of new reaction product observed in Figure 7b corresponds to approximately 10^{-6} mol. This 1 μ mol of product is generated by contacting the TFAAD to $\sim 10^{-9}$ mol of surface atoms from the H-terminated diamond. The 1000-fold difference in these numbers implies that approximately 1000 product molecules are produced in solution for each molecule that ultimately reacts with the surface. Photochemical removal of surface hydrogen by cleavage of the surface C–H bond would directly produce no more than two radicals (one each on the H and the C) for each surface site. In contrast, the ejection of electrons from the surface would create one radical in the liquid for each electron ejected. While it is conceivable that a single C–H cleavage might initiate a branching chain reaction in which one radical leads to formation of multiple radicals, reactions of this type are rare.⁴⁹ A previous study of radicals formed by electron impact on *n*-alkanes concluded that the radicals that were observed were those formed by the initial impact process, with little or no subsequent chemistry.^{50,51} Alkene (olefin) polymerization reactions are widely known to be simple chain reactions in which the number of radicals is constant, and only one polymer molecule is formed for each initiation event.⁵² Thus, this process cannot easily account for the large number of small reaction products detected in solution. Furthermore, we see no evidence for polymer formation in GC-MS or in XPS data. In summary, the XPS, UPS, and GC-MS data all suggest that it is unlikely that photoinduced cleavage of C–H surface bonds can account for the primary reaction pathway.

Instead, the data suggest that ejection of electrons from diamond into the liquid phase is more likely to be responsible for initiating the reaction. The negative electron affinity of the H-terminated samples is significant because it implies that there is no barrier to electron ejection at the surface, so that any process that excites electrons to the conduction band can lead to facile electron emission into vacuum. Indeed, many studies have reported photoelectron ejection from H-terminated diamond, even using sub-band-gap light.^{33,34,53,56} On diamond (111) electron ejection into vacuum has been reported using photons as low as 2.0 eV energy,⁵⁷ with a significant increase in yield for photons with >4.2 eV energy.⁵³

For sub-band-gap illumination, these studies have reported two possible pathways for electron emission: (1) ejection of electrons from the conduction band assisted by surface states or bulk defect states lying within the bulk band gap^{32–35,53} and

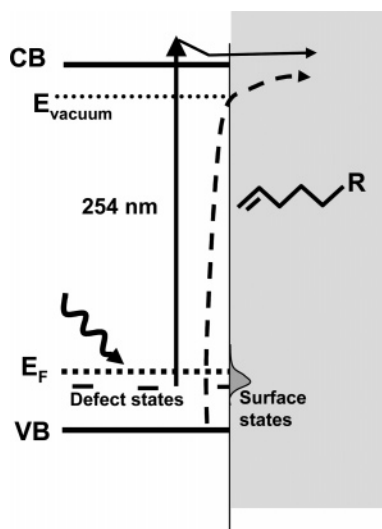


Figure 8. Proposed mechanisms for ejection of electrons into liquid phase: excitation from occupied defects and/or surface states to the conduction band followed by diffusion and emission (solid arrow); direct photoemission from valence band to the vacuum level (dashed arrow).

(2) direct ejection from the valence band to the low-lying vacuum level, without passing through the conduction band.⁵⁸ The second process is inefficient because of momentum conservation rules at the diamond–vacuum interface.⁵⁶ Ejection of electrons is much more efficient when the excitation to the conduction band occurs because in this case it is possible to create excitons deep into the sample that can then diffuse to the surface where they dissociate and eject the electron into vacuum.⁵⁶ In this situation, the importance of NEA is that (1) excitations initiated even at bulk defects can lead to electron emission from the surface and (2) any other excitation that promotes electrons to the conduction band can lead to electron emission. Excitations involving surface states may be particularly effective because of the relaxation of momentum conservation rules. The photoinduced transfer of electrons to molecular species has been previously identified for the photochemical reactions of molecules on metals and semiconductors. On metals, excitation at wavelengths below the work function has been shown to transfer electrons to molecules in an adsorbed layer, where they initiate bond cleavage and desorption of radical species.⁴³ Similarly, illumination of CH_3Br on GaAs(110) at wavelengths several electronvolts below the work function can induce electron transfer to the CH_3Br , which subsequently dissociates.⁴⁵ These studies have established a precedent for direct photoinduced electron-transfer reactions.

Our experimental results show that H–NCD exhibits negative electron affinity, $\chi \sim -0.5$ eV, with the valence band maximum ~ 0.7 eV below the Fermi energy. Excitation of electrons from filled surface states to the conduction band using a single 4.9 eV photon is then possible for the surface/defect states lying within ~ 0.1 eV of the Fermi energy. The valence band photoemission studies show clear evidence for electronic states in this energy range on the H–NCD surface and on a surface partially functionalized with TFAAD. Thus, the conditions needed to emit electrons into the reactant molecular fluid are satisfied. As depicted in Figure 8, our data suggest that the photochemical functionalization is initiated by photoejected electrons produced either (1) by excitation of surface states lying just below the Fermi energy up to the conduction band followed by ejection of an electron into the liquid phase (solid lines) or

(2) by direct ejection of electrons from the valence band to the liquid phase via internal photoemission (dashed line).^{43–45}

Mechanism of Functionalization. Our data strongly suggest that the photochemical functionalization is initiated by the emission of an electron into the liquid phase. In principle, the surface reaction could occur by several subsequent pathways: (1) formation of liquid-phase radical anions that then react directly with the H-terminated sample, (2) formation of liquid-phase radical anions that abstract H atoms from the surface, thereby creating reactive surface sites that covalently bond to other molecules in solution, or (3) formation of positive holes in the surface layer that act as sites for reaction with the alkene functionality. Previous studies have demonstrated that radical initiators such as benzoyl peroxide and lauroyl peroxide can be used to initiate the functionalization of H-terminated diamond with nitriles and carboxylic acids.^{9,59–61} These papers proposed that the radical initiator removes a hydrogen atom from the surface, leaving a dangling bond (surface radical) on the diamond. Additional initiator species in solution then remove H from the target molecule (for example, the acidic H on the $-\text{COOH}$ group of the acid). Recombination of the surface radical with the newly formed target radical then ensues.

We believe a similar process occurs at the diamond surface, in which electrons ejected into solution create radical anions in the liquid. Some of these anions may abstract H atoms from the surface, leaving reactive surface sites that then link to the $\text{C}=\text{C}$ moiety of the liquid-phase molecules, in a manner similar to that observed on silicon surfaces.⁶² A number of studies have shown that dangling bonds created on H-terminated or vacuum-annealed silicon^{63–66} as well as silicon that has been illuminated with short-wavelength UV radiation⁶⁷ act as highly reactive sites that will bind to a wide variety of alkenes. A major difference between the *photochemical* reactions of silicon and diamond is that on silicon the functionalization is initiated with photons whose energy is greater than the energy of the $\text{Si}-\text{H}$ bond, leading to a direct photochemical excitation of the surface. In the case of diamond, the energy of the $\text{C}-\text{H}$ bond leads to a much less direct, and less efficient, reaction pathway.

To maintain overall charge neutrality, the number of electrons ejected must eventually be balanced by an equivalent number of oxidation reactions at the surface. While some of these might involve surface reactions (such as removal of protons from the surface to balance the electrons ejected), others may involve oxidation reactions via transfer of electrons from molecules in the liquid phase back to the valence band of the diamond. This situation is similar to the photocatalytic oxidation on TiO_2 . In that case excitation across the band gap creates holes that oxidize organic molecules; charge neutrality is maintained by the reduction of O_2 , H_2O , or other species at the reaction interface.^{68,69}

The propensity for oxidation vs reduction of the alkenes in solution by the diamond can be qualitatively estimated on the basis of an energy level diagram for the diamond–liquid interface using data in the literature for model compounds, as illustrated in Figure 9. Because relevant parameters are not available for many molecules and because most alkenes are expected to behave rather similarly, we use cyclohexene as a model. For cyclohexene, the electron affinity (EA) is 2.1 eV⁷⁰ and the ionization potential is 9.1 eV.⁷¹ This places the energy of the gas-phase anion 2.1 eV above the vacuum level and the cation 9.1 eV below the vacuum level. In liquid form, the IP and EA are modified by the polarization of the solvent. The polarization energy, sometimes referred to as the Born energy, reflects the additional stabilization of ions due to polarization

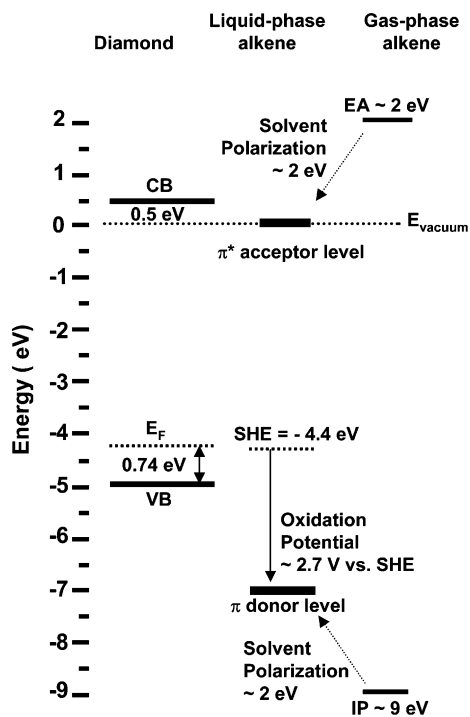


Figure 9. Approximate energy level diagram showing measured positions of diamond band edges and the approximate expected positions of alkene π (electron donor) and π^* (electron acceptor) states in a vacuum (far right) and in liquid (center).

of the surrounding dielectric; it can be estimated by comparing the ionization potential in a vacuum with the electrochemical oxidation potential. For cyclohexene, oxidation occurs at a potential of 2.7 eV with respect to the standard hydrogen electrode (SHE). Since the SHE is known to correspond to an absolute energy of -4.4 eV with respect to vacuum, this means that the oxidation of cyclohexene in liquid form occurs at 7.1 eV relative to the vacuum level. Thus, the polarization of the solvent reduces the energy needed to oxidize cyclohexene by approximately 2 eV, from 9.1 eV in a vacuum to 7.1 eV in solution; this can be represented as the energy of a π donor state lying at -7.1 eV. Similarly, the EA of cyclohexene is 2.1 eV; if the solvation energy is independent of the sign of the charge, then this places the energy of the solvated anion (the π^* acceptor state) essentially at the vacuum level.

One important result from this rough analysis is that it becomes clear that holes in diamond are not very effective at oxidizing alkenes, as the valence band maximum lies several electronvolts above the π donor state of the molecule; holes are more stable in diamond than on the alkene. However, photoexcited diamond should be good at reducing alkenes, as the π^* acceptor state of the alkenes is predicted to lie below the conduction band minimum, near the vacuum level. This observation indicates that, on diamond, the high energy of the conduction band lends itself to reduction of molecules, which if balanced by corresponding oxidation by holes in the conduction band, can easily generate multiple product molecules in solution, in agreement with our experimental results.

While our experiments are not able to establish a detailed mechanism of the radical chemistry in solution, all of our data, especially combined with the extensive prior literature on photoejection of electrons from diamond, strongly suggest that the photochemical functionalization of diamond using 254 nm photons is initiated by an optical excitation process that ejects electrons into the liquid phase.

Conclusions

The photochemical reaction of H-terminated diamond surfaces using alkenes provides a versatile pathway for preparing diamond surfaces with specific chemical functional groups. Valence-band photoemission confirms that the H-terminated surfaces have negative electron affinity, and our results strongly suggest that the photochemical functionalization with alkenes is initiated by the ejection of electrons from the H-terminated surfaces upon illumination with short wavelength UV light. The observation of reaction products in solution only when the TFAAD is illuminated in direct contact with the H-terminated diamond confirms that the reaction must involve optical excitation within the diamond or at its surface to initiate the reaction. The observation of ~ 1000 product molecules in the liquid phase per functionalized surface site and the absence of any significant C–H bond cleavage in ultrahigh vacuum all point to a photochemical process driven by the photoexcited electrons and holes. The ability to functionalize using sub-band-gap illumination is consistent with previous studies demonstrating weak electron emission from sub-band-gap illumination of diamond and likely explains the comparatively low overall rate of reaction. While the negative electron affinity of diamond has long been recognized, the potential implications of this for surface chemistry have not been previously recognized. Since NEA is found on a number of wide band gap semiconducting materials, the mechanistic picture presented here suggests that photoelectron emission may potentially be a versatile way to initiate surface functionalization of these materials.

Acknowledgment. This manuscript is based on research supported by the National Science Foundation Grant CHE-0314618. The authors acknowledge Tatyana Feygelson, Geo-Centers Inc. for growth of diamond films. J.E.B. and J.N.R. acknowledge the support of the Naval Research Laboratory/Office of Naval Research.

Supporting Information Available: XPS and GC-MS data from oxidized diamond samples and results of experiments conducted with addition of nitrobenzene as an electron acceptor to the perfluorodecene (pdf). This material is available free of charge via the Internet at <http://pubs.acs.org>.

References and Notes

- (1) May, P. W. *Philos. Trans. R. Soc. London, Ser. A* **2000**, *358*, 473.
- (2) Railkar, T. A.; Kang, W. P.; Windischmann, H.; Malshe, A. P.; Naseem, H. A.; Davidson, J. L.; Brown, W. D. *Crit. Rev. Solid State Mater. Sci* **2000**, *25*, 163.
- (3) Swain, G. M.; Ramesham, R. *Anal. Chem.* **1993**, *65*, 345.
- (4) Yang, W. S.; Auciello, O.; Butler, J. E.; Cai, W.; Carlisle, J. A.; Gerbi, J. E.; Gruen, D. M.; Knickerbocker, T.; Lasseter, T. L.; Russell, J. N., Jr.; Smith, L. M.; Hamers, R. J. *Nat. Mater.* **2002**, *1*, 253.
- (5) Lu, M. C.; Knickerbocker, T.; Cai, W.; Yang, W. S.; Hamers, R. J.; Smith, L. M. *Biopolymers* **2004**, *73*, 606.
- (6) Yang, W. S.; Butler, J. E.; Russell, J. N., Jr.; Hamers, R. J. *Langmuir* **2004**, *20*, 6778.
- (7) Yang, W. S.; Hamers, R. J. *Appl. Phys. Lett.* **2004**, *85*, 3626.
- (8) Wei, J.; Yates, J. T., Jr. *Crit. Rev. Surf. Chem.* **1995**, *5*, 1.
- (9) Ida, S.; Tsubota, T.; Tanii, S.; Nagata, M.; Matsumoto, Y. *Langmuir* **2003**, *19*, 9693.
- (10) Tsubota, T.; Hirabayashi, O.; Ida, S.; Nagoka, S.; Nagata, M.; Matsumoto, Y. *Diamond Relat. Mater.* **2002**, *11*, 1360.
- (11) Sotowa, K. I.; Amamoto, T.; Sobana, A.; Kusakabe, K.; Imato, T. *Diamond Relat. Mater.* **2004**, *13*, 145.
- (12) Miller, J. B. *Surf. Sci.* **1999**, *439*, 21.
- (13) Liu, Y.; Gu, Z. N.; Margrave, J. L.; Khabashesku, V. N. *Chem. Mater.* **2004**, *16*, 3924.
- (14) Kuo, T. C.; McCreery, R. L.; Swain, G. M. *Electrochem. Solid-State Lett* **1999**, *2*, 288.
- (15) Ohta, R.; Saito, N.; Inoue, Y.; Sugimura, H.; Takai, O. *J. Vac. Sci. Technol., A* **2004**, *22*, 2005.

- (16) Strother, T.; Knickerbocker, T.; Russell, J. N., Jr.; Butler, J. E.; Smith, L. M.; Hamers, R. *J. Langmuir* **2002**, *18*, 968.
- (17) Clare, T. L.; Clare, B. H.; Nichols, B. M.; Abbott, N. L.; Hamers, R. *J. Langmuir* **2005**, *21*, 6344.
- (18) Yang, W. S.; Baker, S. E.; Butler, J. E.; Lee, C. S.; Russell, J. N., Jr.; Shang, L.; Sun, B.; Hamers, R. *J. Chem. Mater.* **2005**, *17*, 938.
- (19) Hartl, A.; Schmich, E.; Garrido, J. A.; Hernando, J.; Catharino, S. C. R.; Walter, S.; Feulner, P.; Kromka, A.; Steinmuller, D.; Stutzmann, M. *Nat. Mater.* **2004**, *3*, 736.
- (20) Butler, J. E.; Windischmann, H. *MRS Bull.* **1998**, *23*, 22.
- (21) Strother, T.; Hamers, R. J.; Smith, L. M. *Nucleic Acids Res.* **2000**, *28*, 3535.
- (22) Schlaf, R.; Schroeder, P. G.; Nelson, M. W.; Parkinson, B. A.; Lee, P. A.; Nebesny, K. W.; Armstrong, N. R. *J. Appl. Phys.* **1999**, *86*, 1499.
- (23) Tse, K.-Y.; Nichols, B. M.; Yang, W.; Butler, J. E.; Russell, J. N., Jr.; Hamers, R. *J. Phys. Chem. B* **2005**, *109*, 8523.
- (24) Powell, C. J.; Jablonski, A. *NIST Electron Inelastic-Mean-Free-Path Database*, Version 1.1; National Institute of Standards and Technology: Gaithersburg, MD, 2000.
- (25) Gries, W. H. *Surf. Interface Anal.* **1996**, *24*, 38.
- (26) Dean, P. J.; Lightowers, E. C.; Wight, D. R. *Phys. Rev.* **1965**, *140*, A352.
- (27) Himpfel, F. J.; Knapp, J. A.; VanVechten, J. A.; Eastman, D. E. *Phys. Rev. B* **1979**, *20*, 624.
- (28) Diederich, L.; Aebi, P.; Kuttel, O. M.; Schlapbach, L. *Surf. Sci.* **1999**, *424*, L314.
- (29) Ley, L.; Graupner, R.; Cui, J. B.; Ristein, J. *Carbon* **1999**, *37*, 793.
- (30) Baumann, P. K.; Nemanich, R. J. *Surf. Sci.* **1998**, *409*, 320.
- (31) van der Weide, J.; Zhang, Z.; Baumann, P. K.; Wensell, M. G.; Bernholz, J.; Nemanich, R. J. *Phys. Rev. B* **1994**, *50*, 5803.
- (32) Ristein, J.; Stein, W.; Ley, L. *Phys. Rev. Lett.* **1997**, *78*, 1803.
- (33) Vouagner, D.; Show, Y.; Kiraly, B.; Champagnon, B.; Girardeau-Montaut, J. P. *Appl. Surf. Sci.* **2000**, *168*, 79.
- (34) Cui, J. B.; Ristein, J.; Ley, L. *Phys. Rev. B* **1999**, *60*, 16135.
- (35) Cui, J. B.; Stammler, M.; Ristein, J.; Ley, L. *J. Appl. Phys.* **2000**, *88*, 3667.
- (36) Mansour, A.; Indlekofer, G.; Oelhafen, P. *Appl. Surf. Sci.* **1991**, *48-49*, 312.
- (37) Diederich, L.; Kuttel, O. M.; Schaller, E.; Schlapbach, L. *Surf. Sci.* **1996**, *349*, 176.
- (38) Baumann, P. K.; Nemanich, R. J. *Diamond Relat. Mater.* **1995**, *4*, 802.
- (39) Bandis, C.; Pate, B. B. *Appl. Phys. Lett.* **1996**, *69*, 366.
- (40) Kawarada, H. *Surf. Sci. Rep.* **1996**, *26*, 205.
- (41) Pate, B. B. *Surf. Sci.* **1986**, *165*, 83.
- (42) Cui, J. B.; Ristein, J.; Ley, L. *Phys. Rev. Lett.* **1998**, *81*, 429.
- (43) Cho, C.-C.; Collings, B. A.; Hammer, R. E.; Polanyi, J. C.; Stanners, C. D.; Wang, J. H.; Xu, G.-Q. *J. Phys. Chem.* **1989**, *93*, 7761.
- (44) Khan, K. A.; Camillone, N.; Yarmoff, J. A.; Osgood, R. M., Jr. *Surf. Sci.* **2000**, *458*, 53.
- (45) Yang, Q.; Osgood, R. M., Jr. *J. Phys. Chem.* **1993**, *97*, 8855.
- (46) Cicero, R. L.; Linford, M. R.; Chidsey, C. E. D. *Langmuir* **2000**, *16*, 5688.
- (47) Nuzzo, R. G.; Allara, D. L. *J. Am. Chem. Soc.* **1983**, *105*, 4481.
- (48) Smith, M. B.; March, J. *March's Advanced Organic Chemistry: Reactions, Mechanism, and Structure*, 5th ed.; Wiley-Interscience: New York, 2001.
- (49) Troe, J. *Annu. Rev. Phys. Chem.* **1978**, *29*, 223.
- (50) Wojnarovits, L.; Schuler, R. H. *J. Phys. Chem. A* **2000**, *104*, 1346.
- (51) Belevskii, V. N.; Belopushkin, S. I. *High Energy Chem.* **2005**, *39*, 5.
- (52) Stevens, M. P. *Polymer Chemistry*; Oxford University Press: New York, 1999.
- (53) Ristein, J.; Stein, W.; Ley, L. *Diamond Relat. Mater.* **1998**, *7*, 626.
- (54) Orlanducci, S.; Sessa, V.; Terranova, M. L.; Tazzioli, F.; Vicario, C.; Boscolo, I.; Cialdi, S.; Catani, L.; Rossi, M. *Diamond Relat. Mater.* **2003**, *12*, 2186.
- (55) Rouse, A. A.; Bernhard, J. B.; Sosa, E. D.; Golden, D. E. *Appl. Phys. Lett.* **1999**, *75*, 3417.
- (56) Bandis, C.; Pate, B. B. *Phys. Rev. Lett.* **1995**, *74*, 777.
- (57) Cui, J. B.; Ristein, J.; Ley, L. *Diamond Relat. Mater.* **2000**, *9*, 1036.
- (58) Takeuchi, D.; Kato, H.; Ri, G. S.; Yamada, T.; Vinod, P. R.; Hwang, D.; Nebel, C. E.; Okushi, H.; Yamasaki, S. *Appl. Phys. Lett.* **2005**, *86*, 152103.
- (59) Tsubota, T.; Ida, S.; Hirabayashi, O.; Nagaoka, S.; Nagata, M.; Matsumoto, Y. *Phys. Chem. Chem. Phys.* **2002**, *4*, 3881.
- (60) Tsubota, T.; Tanii, S.; Ida, S.; Nagata, M.; Matsumoto, Y. *Diamond Relat. Mater.* **2004**, *13*, 1093.
- (61) Tsubota, T.; Tanii, S.; Ida, S.; Nagata, M.; Matsumoto, Y. *Phys. Chem. Chem. Phys.* **2003**, *5*, 1474.
- (62) Cicero, R. L.; Chidsey, C. E. D.; Lopinski, G. P.; Wayner, D. D. M.; Wolkow, R. A. *Langmuir* **2002**, *18*, 305.
- (63) Hovis, J. S.; Hamers, R. J. *J. Phys. Chem. B* **1998**, *102*, 687.
- (64) Lopinski, G. P.; Moffatt, D. J.; Wayner, D. D. M.; Wolkow, R. A. *J. Am. Chem. Soc.* **2000**, *122*, 3548.
- (65) Lua, Y. Y.; Fillmore, W. J. J.; Linford, M. R. *Appl. Surf. Sci.* **2004**, *231-2*, 323.
- (66) Schwartz, M. P.; Hamers, R. J. *Surf. Sci.* **2002**, *515*, 75.
- (67) Linford, M. R.; Fenter, P.; Eisenberger, P. M.; Chidsey, C. E. D. *J. Am. Chem. Soc.* **1995**, *117*, 3145.
- (68) Lu, G.; Linsebigler, A.; Yates, J. T., Jr. *J. Phys. Chem.* **1995**, *99*, 7626.
- (69) Zhuang, J.; Rusu, C. N.; Yates, J. T., Jr. *J. Phys. Chem. B* **1999**, *103*, 6957.
- (70) Jordan, K. D.; Michejda, J. A.; Burrow, P. D. *Chem. Phys. Lett.* **1976**, *42*, 227.
- (71) Fleischmann, M.; Pletcher, D. *Tetrahedron Lett.* **1968**, *9*, 6255.